

SLAC-PUB-8198
July 1999

PERSPECTIVES ON EPIC PHYSICS*

Stanley J. Brodsky
Stanford Linear Accelerator Center
Stanford University, Stanford, California 94309
email: sjbth@slac.stanford.edu

Abstract

An electron-proton/ion polarized beam collider (EPIC) with high luminosity and center of mass energy $\sqrt{s} = 25$ GeV would be a valuable facility for fundamental studies of proton and nuclear structure and tests of quantum chromodynamics, I review a sample of prospective EPIC topics, particularly semi-exclusive reactions, studies of the proton fragmentation region, heavy quark electroproduction, and a new probe of odderon/pomeron interference.

Talk presented at the
EPIC'99 Workshop
Indiana University Cyclotron Facility
Bloomington, Indiana
April 8–11, 1999

*Work supported by the Department of Energy, contract DE-AC03-76SF00515.

1 Introduction

A central goal of both high energy and nuclear physics is to unravel the structure and dynamics of nucleons and nuclei in terms of their fundamental quark and gluon degrees of freedom. An outstanding option for such experimental studies is an electron-proton/ion polarized beam collider (EPIC) in an intermediate energy domain well above the fixed target facilities available at Jefferson Laboratory or SLAC, and well below the high energy range of the electron-proton collider HERA at DESY. For example, an electron beam of 4 GeV colliding with protons or ions at 40 GeV would provide center-of-mass energies $\sqrt{s} \cong 25$ GeV, well above both the open charm and bottom thresholds and well-matched to QCD studies. The equivalent electron laboratory beam energy is $E_{\text{Lab}}^e \cong 300$ GeV. The EPIC collider is envisioned to have polarized beams and high luminosity, $\mathcal{L} \cong 10^{33} \text{cm}^{-2} \text{sec}^{-1}$. With good duty factor for studying exclusive final states and multiparticle correlations, and with full angular acceptance,—especially in the beam fragmentation region—the EPIC facility would constitute a complete “electron microscope” for testing QCD and illuminating hadron and nuclear substructure.

Our present empirical knowledge of the quark and gluon distributions of the proton has revealed a remarkably complex substructure. It is helpful to categorize parton distributions as “intrinsic” —pertaining to the composition of the target hadron, and “extrinsic”, reflecting the resolved PQCD substructure of the individual quarks and gluons themselves. For example, If sea quarks were generated solely by gluon splitting, the anti-quark distributions would be isospin symmetric. However, the $\bar{u}(x)$ and $\bar{d}(x)$ antiquark distributions of the proton at $Q^2 \sim 10 \text{ GeV}^2$ have quite different shapes, which must reflect dynamics intrinsic to the proton’s structure. We now know that gluons carry a significant fraction of the proton’s spin as well as its momentum. Since gluon exchange between valence quarks contributes to the $p - \Delta$ mass splitting, it follows that the gluon distributions cannot be solely accounted for by bremsstrahlung from individual quarks. Similarly, in the case of heavy quarks, $s\bar{s}$, $c\bar{c}$, $b\bar{b}$, the diagrams in which the sea quarks are multiply-connected to the proton’s valence quarks are intrinsic to the proton’s structure itself. Thus neither gluons nor sea quarks are solely generated by DGLAP evolution, and one cannot define a resolution scale in momentum transfer in deep inelastic scattering Q_0 where the sea or gluon degrees of freedom can be neglected. There are also remarkable surprises associated with the chirality distributions of the quarks $\Delta q = q_{\uparrow/\uparrow} - q_{\downarrow/\uparrow}$ of

the valence quark $\Delta u(x, Q)$ and $\Delta d(x, Q)$, which again show that a simple valence quark approximation to nucleon spin structure functions is far from the actual dynamical situation.

An electron-proton/ion collider in the EPIC energy regime would clearly be a valuable facility for many types of QCD studies. A large array of such topics were discussed in this workshop. Examples include:

1. The polarized beams of EPIC would provide the capability for studying detailed spin and azimuthal correlations, reflecting the helicity distributions of the quark and gluon constituents and the physics of spin transfer to the final state hadrons in the jet beam fragmentation region.[1]
2. The study of the proton fragmentation regime; *i.e.* the observation of the remnants of the disassociated proton left behind after a struck is struck. Veneziano and Trentadue [2] have emphasized the proton's "fracture functions" arising from the evolution of the target fragments with Q^2 . More generally, the physics of the fragmentation region, even Coulomb dissociation, reflects the actual composition of the light-cone wave functions of hadrons and nuclei, a largely unexplored area of QCD which could provide important insights into the fundamental structure of the nucleon.
3. The study of the interface of coherent and incoherent quark phenomena. This includes the large $x \rightarrow 1$ regime where perturbative QCD predicts specific power-law fall off of scattering amplitudes and one expects duality between exclusive and inclusive channels. Further, one can study "semi-exclusive" reactions such as $\gamma^* p \rightarrow \pi^+ X$ where the meson is produced at large transverse momentum in isolation of other hadrons, *i.e.* a large rapidity gap.[3, 4] Such reactions provide the capability of designing effective currents which probe specific parton distributions.
4. The study of purely exclusive reactions, such as large momentum transfer fixed-angle reactions, meson photoproduction, processes which all depend in detail on hadron distribution amplitudes $\phi_H(x_i, Q)$, the basic wavefunctions of the hadrons.[5, 6]
5. The study of diffractive processes where the interacting proton or nucleus remains intact, such as deeply virtual Compton scattering, $\gamma^* p \rightarrow \gamma p$, diffractive meson electroproduction $\gamma^* p \rightarrow \phi p$, $\gamma^* p \rightarrow \pi^0 p$ processes

which are sensitive to the dynamics of the QCD hard pomeron and odderon, the $C = +1$, and -1 exchange systems which control high energy scattering. Measurements of diffractive dijet production $\gamma^*p \rightarrow \text{Jet Jet } p$ test the QCD structure of virtual photons. The charge asymmetry in $\gamma^*p \rightarrow c\bar{c}p$ measures pomeron/odderon interference and has high sensitivity to the odderon amplitude.[7]

6. The nuclear beam capability of the EPIC collider is important for identifying basic and novel features of fundamental nuclear dynamics, such as color transparency, hidden color, and specific dynamics associated with the non-additive “EMC” features of nuclear structure functions. Color transparency[8, 9] reflects the fact that hadrons are fluctuating systems, and that only the small transverse size valence quark components of the hadron wavefunctions enter virtual photoproduction processes such as $\gamma^*A \rightarrow \rho^0 A'$, and hard quasi-elastic processes such as $eA \rightarrow e'p(A-1)$. Such compact wavefunctions are predicted to have minimal shadowing and other hadronic interactions. The first evidence for QCD “color transparency” was observed in quasi-elastic pp scattering in nuclei.[10] In contrast to color transparency, Fock states with large-scale color configurations interact strongly and with high particle number production. [11]
7. Hidden color is a fundamental prediction of QCD, reflecting the fact that the nuclear wavefunction cannot be solely described as composite of nucleon color singlet configurations.[12] Such components should show up in non-additivity of nuclear amplitudes as well as the complex structure of the nuclear fragmentation region.
8. The energy range of the EPIC facility would allow a detailed study of heavy quark phenomena associated with nucleon structure, such as the charm and bottom structure functions over the full range of x_{bj} . The EMC experiment measured a charm structure function at large x_{bj} and Q^2 much larger than expected from photon gluon fusion, indicating an intrinsic charm content[13] of the proton with probability $P_{c\bar{c}} \cong 0.6 \pm 0.3\%$. [14] The intrinsic heavy quark wavefunction is maximal at equal rapidity; *i.e.* light-cone momentum fractions

$$k_i^+/p^+ \cong x_{\perp i} / \sum_j x_{\perp j} \quad (1)$$

predicting charm and bottom distributions at large x_{bj} and leading heavy hadrons at large x_F in the proton fragmentation region. These novel features would be well-studied in a collider such as EPIC.

9. The full range of Compton processes would be accessible, including exclusive virtual Compton scattering and Compton/Bethe-Heitler interference $\gamma^*p \rightarrow \gamma p'$ and $\gamma^*p \rightarrow \gamma^*p'$;[15, 16] and inclusive deep inelastic Compton scattering $\gamma p \rightarrow \gamma X$ and $\gamma p \rightarrow \gamma^*p$ which can be used to measure new quark distributions and sum rules weighted by the quark charge e_q^4 or e_q^3 . [17]

The common denominator in all of these QCD studies is the hadron light-cone wavefunction; the boost-invariant amplitude which represents the hadron in terms of its quark and gluon quanta. In the next section I will review some of the universal features of light-cone wavefunctions, and in the following sections, I will review in more detail specific EPIC topics.

2 QCD Phenomena at EPIC and the Light-Cone Wavefunctions of Hadrons

In a relativistic collision, the incident hadron projectile presents itself as an ensemble of coherent states containing various numbers of quark and gluon quanta. Thus when the electron in an electron-proton collider crosses a proton at fixed “light-cone” time $\tau = t + z/c = x^0 + x^z$, it encounters a baryonic state with a given number of quarks, anti-quarks, and gluons in flight with $n_q - n_{\bar{q}} = 3$. The natural framework for describing these hadronic components in QCD at the amplitude level is the light-cone Fock representation obtained by quantizing the theory at fixed τ . [18] For example, the proton state has the Fock expansion

$$\begin{aligned}
 |p\rangle &= \sum_n \langle n | p \rangle |n\rangle \\
 &= \psi_{3q/p}^{(\Lambda)}(x_i, \vec{k}_{\perp i}, \lambda_i) |uud\rangle \\
 &\quad + \psi_{3qg/p}^{(\Lambda)}(x_i, \vec{k}_{\perp i}, \lambda_i) |uudg\rangle + \dots
 \end{aligned} \tag{2}$$

representing the expansion of the exact QCD eigenstate on a non-interacting quark and gluon basis. The probability amplitude for each such n -particle

state of on-mass shell quarks and gluons in a hadron is given by a light-cone Fock state wavefunction $\psi_{n/H}(x_i, \vec{k}_{\perp i}, \lambda_i)$, where the constituents have longitudinal light-cone momentum fractions

$$x_i = \frac{k_i^+}{p^+} = \frac{k^0 + k_i^z}{p^0 + p^z}, \quad \sum_{i=1}^n x_i = 1, \quad (3)$$

relative transverse momentum

$$\vec{k}_{\perp i}, \quad \sum_{i=1}^n \vec{k}_{\perp i} = \vec{0}_{\perp}, \quad (4)$$

and helicities λ_i . The effective lifetime of each configuration in the laboratory frame is $2P_{lab}/\mathcal{M}_n^2 - M_p^2$ where

$$\mathcal{M}_n^2 = \sum_{i=1}^n \frac{k_{\perp i}^2 + m^2}{x} < \Lambda^2 \quad (5)$$

is the off-shell invariant mass and Λ is a global ultraviolet regulator. The form of the $\psi_{n/H}^{(\Lambda)}(x_i, \vec{k}_{\perp i}, \Lambda_c)$ is invariant under longitudinal boosts; *i.e.*, the light-cone wavefunctions expressed in the relative coordinates x_i and $k_{\perp i}$ are independent of the total momentum P^+ , \vec{P}_{\perp} of the hadron.

Thus the interactions of the proton reflects an average over the interactions of its fluctuating states. For example, a valence state with small impact separation, and thus a small color dipole moment, would be expected to interact weakly in a hadronic or nuclear target reflecting its color transparency. The nucleus thus filters differentially different hadron components.[19, 20] The ensemble $\{\psi_{n/H}\}$ of such light-cone Fock wavefunctions is a key concept for hadronic physics, providing a conceptual basis for representing physical hadrons (and also nuclei) in terms of their fundamental quark and gluon degrees of freedom. Given the $\psi_{n/H}^{(\Lambda)}$, we can construct any spacelike electromagnetic or electroweak form factor from the diagonal overlap of the LC wavefunctions.[21] In the case of semileptonic decays of heavy mesons, one also obtains important contributions from LC Fock states with $\Delta n = 2$. [22] Similarly, the matrix elements of the currents that define quark and gluon structure functions can be computed from the integrated squares of the LC wavefunctions.[5]

It is thus important not only to compute the spectrum of hadrons and gluonic states, but also to determine the wavefunction of each QCD bound

state in terms of its fundamental quark and gluon degrees of freedom. If we could obtain such nonperturbative solutions of QCD, then we would be able to compute from first principles the quark and gluon structure functions and distribution amplitudes which control hard-scattering inclusive and exclusive reactions as well as calculate the matrix elements of currents which underlie electroweak form factors and the weak decay amplitudes of the light and heavy hadrons. The light-cone wavefunctions also determine the multiparton correlations which control the distribution of particles in the proton fragmentation region as well as dynamical higher twist effects. Thus one can analyze not only the deep inelastic structure functions but also the fragmentation of the proton spectator system. Knowledge of hadron wavefunctions would also open a window to a deeper understanding of the physics of QCD at the amplitude level, illuminating exotic effects of the theory such as color transparency, intrinsic heavy quark effects, hidden color, diffractive processes, and the QCD van der Waals interactions.

Solving a quantum field theory such as QCD is clearly not easy. However, highly non-trivial, one-space one-time relativistic quantum field theories which mimic many of the features of QCD, have already been completely solved using light-cone Hamiltonian methods.[18] Virtually any (1+1) quantum field theory can be solved using the method of Discretized Light-Cone Quantization (DLCQ).[23, 24] In DLCQ, the Hamiltonian H_{LC} , which can be constructed from the Lagrangian using light-cone time quantization, is completely diagonalized, in analogy to Heisenberg's solution of the eigenvalue problem in quantum mechanics. The quantum field theory problem is rendered discrete by imposing periodic or anti-periodic boundary conditions. The eigenvalues and eigensolutions of collinear QCD then give the complete spectrum of hadrons, nuclei, and gluonium and their respective light-cone wavefunctions.

The existence of an exact formalism provides a basis for systematic approximations. For example, one can analyze exclusive processes which involve hard internal momentum transfer using a perturbative QCD formalism patterned after the analysis of form factors at large momentum transfer.[5] The hard-scattering analysis proceeds by writing each hadronic wavefunction as a sum of soft and hard contributions $\psi_n = \psi_n^{\text{soft}}(\mathcal{M}_n^2 < \Lambda^2) + \psi_n^{\text{hard}}(\mathcal{M}_n^2 > \Lambda^2)$, where \mathcal{M}_n^2 is the invariant mass of the partons in the n -particle Fock state and Λ is the separation scale. The high internal momentum contributions to the wavefunction ψ_n^{hard} can be calculated systematically from QCD perturbation theory by iterating the gluon exchange kernel. The contributions from

high momentum transfer amplitude can then be written as a convolution of a hard scattering quark-gluon scattering amplitude T_H with the distribution amplitudes $\phi(x_i, \Lambda)$, the valence wavefunctions obtained by integrating the constituent momenta up to the separation scale $\mathcal{M}_n < \Lambda < Q$. This is the basis for the perturbative hard scattering analyses.[25, 26, 27, 28] In the exact analysis, one can identify the hard PQCD contribution as well as the soft contribution from the convolution of the light-cone wavefunctions. Furthermore, the hard scattering contribution can be systematically improved. For example, off-shell effects can be retained in the evaluation of T_H by utilizing the exact light-cone energy denominators.

More generally, hard exclusive hadronic amplitudes such as quarkonium decay, heavy hadron decay, and scattering amplitudes such as deeply virtual Compton scattering can be written as the convolution of the light-cone Fock state wavefunctions with quark-gluon matrix elements [5]

$$\begin{aligned} \mathcal{M}_{\text{Hadron}} = & \prod_H \sum_n \int \prod_{i=1}^n d^2 k_{\perp} \prod_{i=1}^n dx \delta \left(1 - \sum_{i=1}^n x_i \right) \delta \left(\sum_{i=1}^n \vec{k}_{\perp i} \right) \\ & \times \psi_{n/H}^{(\Lambda)}(x_i, \vec{k}_{\perp i}, \Lambda_i) T_H^{(\Lambda)} . \end{aligned} \quad (6)$$

Here $T_H^{(\Lambda)}$ is the underlying quark-gluon subprocess scattering amplitude, where the (incident or final) hadrons are replaced by quarks and gluons with momenta $x_i p^+$, $x_i \vec{p}_{\perp} + \vec{k}_{\perp i}$ and invariant mass above the separation scale $\mathcal{M}_n^2 > \Lambda^2$. The essential part of the wavefunction is the hadronic distribution amplitudes, [5] defined as the integral over transverse momenta of the valence (lowest particle number) Fock wavefunction; *e.g.* for the pion

$$\phi_{\pi}(x_i, Q) \equiv \int d^2 k_{\perp} \psi_{q\bar{q}/\pi}^{(Q)}(x_i, \vec{k}_{\perp i}, \lambda) \quad (7)$$

where the global cutoff Λ is identified with the resolution Q . The distribution amplitude controls leading-twist exclusive amplitudes at high momentum transfer, and it can be related to the gauge-invariant Bethe-Salpeter wavefunction at equal light-cone time $\tau = x^+$. The $\log Q$ evolution of the hadron distribution amplitudes $\phi_H(x_i, Q)$ can be derived from the perturbatively-computable tail of the valence light-cone wavefunction in the high transverse momentum regime.[5] In general the LC ultraviolet regulators provide a factorization scheme for elastic and inelastic scattering, separating the hard dynamical contributions with invariant mass squared $\mathcal{M}^2 > \Lambda_{\text{global}}^2$ from the

soft physics with $\mathcal{M}^2 \leq \Lambda_{\text{global}}^2$ which is incorporated in the nonperturbative LC wavefunctions. The DGLAP evolution of quark and gluon distributions can also be derived by computing the variation of the Fock expansion with respect to Λ^2 . [5]

Given the solution for the hadronic wavefunctions $\psi_n^{(\Lambda)}$ with $\mathcal{M}_n^2 < \Lambda^2$, one can construct the wavefunction in the hard regime with $\mathcal{M}_n^2 > \Lambda^2$ using projection operator techniques. [5] The construction can be done perturbatively in QCD since only high invariant mass, far off-shell matrix elements are involved. One can use this method to derive the physical properties of the LC wavefunctions and their matrix elements at high invariant mass. Since $\mathcal{M}_n^2 = \sum_{i=1}^n \left(\frac{k_i^2 + m^2}{x} \right)_i$, this method also allows the derivation of the asymptotic behavior of light-cone wavefunctions at large k_\perp , which in turn leads to predictions for the fall-off of form factors and other exclusive matrix elements at large momentum transfer, such as the quark counting rules for predicting the nominal power-law fall-off of two-body scattering amplitudes at fixed θ_{cm} . [5] The phenomenological successes of these rules can be understood within QCD if the coupling $\alpha_V(Q)$ freezes in a range of relatively small momentum transfer. [29]

3 Measurement of Light-Cone Wavefunctions via Diffractive Dissociation

Diffractive multi-jet production in heavy nuclei provides a novel way to measure the shape of the LC Fock state wavefunctions and test color transparency. For example, consider the reaction [19, 20] $\pi A \rightarrow \text{Jet}_1 + \text{Jet}_2 + A'$ at high energy where the nucleus A' is left intact in its ground state. The transverse momenta of the jets have to balance so that $\vec{k}_{\perp 1} + \vec{k}_{\perp 2} = \vec{q}_\perp < \mathcal{R}_A^{-1}$, and the light-cone longitudinal momentum fractions have to add to $x_1 + x_2 \sim 1$ so that $\Delta p_L < R_A^{-1}$. The process can then occur coherently in the nucleus. Because of color transparency, i.e., the cancelation of color interactions in a small-size color-singlet hadron, the valence wavefunction of the pion with small impact separation will penetrate the nucleus with minimal interactions, diffracting into jet pairs. [19] The $x_1 = x$, $x_2 = 1 - x$ dependence of the di-jet distributions will thus reflect the shape of the pion distribution amplitude; the $\vec{k}_{\perp 1} - \vec{k}_{\perp 2}$ relative transverse momenta of the jets also gives key information on the underlying shape of the valence pion wavefunction. The QCD

analysis[20] can be confirmed by the observation that the diffractive nuclear amplitude extrapolated to $t = 0$ is linear in nuclear number A , as predicted by QCD color transparency. The integrated diffractive rate should scale approximately as $A^2/R_A^2 \sim A^{4/3}$. A diffractive dissociation experiment of this type, E791, is now in progress at Fermilab using 500 GeV incident pions on nuclear targets.[30] The preliminary results from E791 appear to be consistent with color transparency. The momentum fraction distribution of the jets is consistent with a valence light-cone wavefunction of the pion consistent with the shape of the asymptotic distribution amplitude, the asymptotic solution [5] $\phi_\pi^{\text{asympt}}(x) = \sqrt{3}f_\pi x(1-x)$ to the perturbative QCD evolution equation. Data from CLEO for the $\gamma\gamma^* \rightarrow \pi^0$ transition form factor also favor a form for the pion distribution amplitude close to this form.[31, 32, 29] Conversely, one can use incident real and virtual photons: $\gamma^*A \rightarrow \text{Jet}_1 + \text{Jet}_2 + A'$ to at EPIC confirm the shape of the calculable light-cone wavefunction for transversely-polarized and longitudinally-polarized virtual photons. Such experiments will open up a remarkable, direct window on the amplitude structure of hadrons at short distances. Most interesting, one can use the EPIC electron beam to diffractively dissociate the proton beam into three high p_T jets in the proton fragmentation region $ep \rightarrow e'\mathcal{J}_1\mathcal{J}_2\mathcal{J}_3$ reflecting the high transverse momentum components of the valance proton wavefunction.[20]

4 Other Applications of Light-Cone Quantization to EPIC QCD Phenomenology

Diffractive vector meson photoproduction. The light-cone Fock wavefunction representation of hadronic amplitudes provides a simple eikonal analysis of diffractive high energy processes, such as $\gamma^*(Q^2)p \rightarrow \rho p$, in terms of the virtual photon and the vector meson Fock state light-cone wavefunctions convoluted with the $gp \rightarrow gp$ near-forward matrix element.[33] One can easily show that only small transverse size $b_\perp \sim 1/Q$ of the vector meson distribution amplitude is involved. The hadronic interactions are minimal, and thus the $\gamma^*(Q^2)N \rightarrow \rho N$ reaction can occur coherently throughout a nuclear target in reactions without absorption or shadowing. The $\gamma^*A \rightarrow VA$ process thus provides a natural framework for testing QCD color transparency.[8] Evidence for color transparency in such reactions has been found by Fermilab experiment E665.

Regge behavior of structure functions. The light-cone wavefunctions $\psi_{n/H}$ of a hadron are not independent of each other, but rather are coupled via the equations of motion. Antonuccio, Dalley and I [34] have used the constraint of finite “mechanical” kinetic energy to derive “ladder relations” which interrelate the light-cone wavefunctions of states differing by one or two gluons. We then use these relations to derive the Regge behavior of both the polarized and unpolarized structure functions at $x \rightarrow 0$, extending Mueller’s derivation of the BFKL hard QCD pomeron from the properties of heavy quarkonium light-cone wavefunctions at large N_C QCD.[35]

Structure functions at large x_{bj} . The behavior of structure functions where one quark has the entire momentum requires the knowledge of LC wavefunctions with $x \rightarrow 1$ for the struck quark and $x \rightarrow 0$ for the spectators. This is a highly off-shell configuration, and thus one can rigorously derive quark-counting and helicity-retention rules for the power-law behavior of the polarized and unpolarized quark and gluon distributions in the $x \rightarrow 1$ endpoint domain.[5] It is interesting to note that the evolution of structure functions is minimal in this domain because the struck quark is highly virtual as $x \rightarrow 1$; *i.e.* the starting point Q_0^2 for evolution cannot be held fixed, but must be larger than a scale of order $(m^2 + k_\perp^2)/(1 - x)$.[5, 36]

Intrinsic gluon and heavy quarks. The main features of the heavy sea quark-pair contributions of the Fock state expansion of light hadrons can also be derived from perturbative QCD, since \mathcal{M}_n^2 grows with m_Q^2 . One identifies two contributions to the heavy quark sea, the “extrinsic” contributions which correspond to ordinary gluon splitting, and the “intrinsic” sea which is multi-connected via gluons to the valence quarks. The intrinsic sea is thus sensitive to the hadronic bound state structure.[13] The maximal contribution of the intrinsic heavy quark occurs at $x_Q \simeq m_\perp / \sum_i m_\perp i$ where $m_\perp = \sqrt{m^2 + k_\perp^2}$; *i.e.* at large x_Q , since this minimizes the invariant mass \mathcal{M}_n^2 . The measurements of the charm structure function by the EMC experiment are consistent with intrinsic charm at large x in the nucleon with a probability of order $0.6 \pm 0.3\%$.[14] Similarly, one can distinguish intrinsic gluons which are associated with multi-quark interactions and extrinsic gluon contributions associated with quark substructure.[37] One can also use this framework to isolate the physics of the anomaly contribution to the Ellis-Jaffe sum rule.

Materialization of far-off-shell configurations. In a high energy hadronic collisions, the highly-virtual states of a hadron can be materialized into physi-

cal hadrons simply by the soft interaction of any of the constituents.[38] Thus a proton state with intrinsic charm $|uud\bar{c}c\rangle$ can be materialized, producing a J/ψ at large x_F , by the interaction of the electron with the proton beam.

Comover phenomena. Light-cone wavefunctions describe not only the partons that interact in a hard subprocess but also the associated partons freed from the projectile. The projectile partons which are comoving (*i.e.*, which have similar rapidity) with final state quarks and gluons can interact strongly producing (a) leading particle effects, such as those seen in open charm hadroproduction; (b) suppression of quarkonium[39] in favor of open heavy hadron production, as seen in the E772 experiment; (c) changes in color configurations and selection rules in quarkonium hadroproduction, as has been emphasized by Hoyer and Peigne.[40] All of these effects violate the usual ideas of factorization for inclusive reactions. More than one parton from the projectile can enter the hard subprocess, producing dynamical higher twist contributions, as seen for example in Drell-Yan experiments.[41, 42]

Asymmetric sea. In conventional studies of the “sea” quark distributions, it is usually assumed that, aside from the effects due to antisymmetrization with valence quarks, the quark and antiquark sea contributions have the same momentum and helicity distributions. However, the ansatz of identical quark and anti-quark sea contributions has never been justified, either theoretically or empirically. Obviously the sea distributions which arise directly from gluon splitting in leading twist are necessarily CP-invariant; *i.e.*, they are symmetric under quark and antiquark interchange. However, the initial distributions which provide the boundary conditions for QCD evolution need not be symmetric since the nucleon state is itself not CP-invariant. Only the global quantum numbers of the nucleon must be conserved. The intrinsic sources of strange (and charm) quarks reflect the wavefunction structure of the bound state itself; accordingly, such distributions would not be expected to be CP symmetric.[43, 44] Thus the strange/anti-strange asymmetry of nucleon structure functions provides a direct window into the quantum bound-state structure of hadronic wavefunctions.

Quark and antiquark asymmetry is also implied by a light-cone meson-baryon fluctuation model of intrinsic $q\bar{q}$ pairs.[43] The most important fluctuations are those closest to the energy shell with minimal invariant mass. For example, the coupling of a proton to a virtual $K^+\Lambda$ pair provides a specific source of intrinsic strange quarks and antiquarks in the proton. Since the s and \bar{s} quarks appear in different configurations in the lowest-lying hadronic pair states, their helicity and momentum distributions are distinct.

Such fluctuations are necessarily part of any quantum-mechanical description of the hadronic bound state in QCD and have also been incorporated into the cloudy bag model and Skyrme solutions to chiral theories. Ma and I [44] have utilized a boost-invariant light-cone Fock state description of the hadron wavefunction which emphasizes multi-parton configurations of minimal invariant mass. We find that such fluctuations predict a striking sea quark and antiquark asymmetry in the corresponding momentum and helicity distributions in the nucleon structure functions. In particular, the strange and anti-strange distributions in the nucleon generally have completely different momentum and spin characteristics. For example, the model predicts that the intrinsic d and s quarks in the proton sea are negatively polarized, whereas the intrinsic \bar{d} and \bar{s} antiquarks provide zero contributions to the proton spin. We also predict that the intrinsic charm and anticharm helicity and momentum distributions are not strictly identical. The above picture of quark and antiquark asymmetry in the momentum and helicity distributions of the nucleon sea quarks has support from a number of experimental observations, and we suggest processes to test and measure this quark and antiquark asymmetry in the nucleon sea.

In addition, one could identify dynamical higher twist processes where the electron recoils against two quarks versus one quark by studying the pattern of jet and dijet production in the current and proton beam fragmentation region.

Hidden Color The deuteron form factor at high Q^2 is sensitive to wavefunction configurations where all six quarks overlap within an impact separation $b_{\perp i} < \mathcal{O}(1/Q)$; the leading power-law fall off predicted by QCD is $F_d(Q^2) = f(\alpha_s(Q^2))/(Q^2)^5$, where, asymptotically, $f(\alpha_s(Q^2)) \propto \alpha_s(Q^2)^{5+2\gamma}$.

[45, 12] In general, the six-quark wavefunction of a deuteron is a mixture of five different color-singlet states. The dominant color configuration at large distances corresponds to the usual proton-neutron bound state. However at small impact space separation, all five Fock color-singlet components eventually acquire equal weight, *i.e.*, the deuteron wavefunction evolves to 80% “hidden color.” The relatively large normalization of the deuteron form factor observed at large Q^2 points to sizable hidden color contributions.[46]

Spin-Spin Correlations in Nucleon-Nucleon Scattering and the Charm Threshold One of the most striking anomalies in elastic proton-proton scattering is the large spin correlation A_{NN} observed at large angles.[47] At $\sqrt{s} \simeq 5$ GeV, the rate for scattering with incident proton spins parallel

and normal to the scattering plane is four times larger than that for scattering with anti-parallel polarization. This strong polarization correlation can be attributed to the onset of charm production in the intermediate state at this energy.[48] The intermediate state $|uud\bar{u}udc\bar{c}\rangle$ has odd intrinsic parity and couples to the $J = S = 1$ initial state, thus strongly enhancing scattering when the incident projectile and target protons have their spins parallel and normal to the scattering plane. The charm threshold can also explain the anomalous change in color transparency observed at the same energy in quasi-elastic pp scattering. A crucial test is the observation of open charm production near threshold with a cross section of order of $1\mu\text{b}$. One can also expect similar strong spin-spin correlations at the threshold for charm and bottom production in photon-proton collisions at EPIC.

5 Semi-Exclusive Processes: New Probes of Hadron Structure at EPIC

A new class of hard “semi-exclusive” processes of the form $A + B \rightarrow C + Y$, have been proposed as new probes of QCD.[49, 3, 4] These processes are characterized by a large momentum transfer $t = (p_A - p_C)^2$ and a large rapidity gap between the final state particle C and the inclusive system Y . Here A, B and C can be hadrons or (real or virtual) photons. The cross sections for such processes factorize in terms of the distribution amplitudes of A and C and the parton distributions in the target B . Because of this factorization semi-exclusive reactions provide a novel array of generalized currents, which not only give insight into the dynamics of hard scattering QCD processes, but also allow experimental access to new combinations of the universal quark and gluon distributions. These are ideal processes to study at EPIC.

QCD scattering amplitudes for deeply virtual exclusive processes such as Compton scattering $\gamma^*p \rightarrow \gamma p$ and meson production $\gamma^*p \rightarrow Mp$ factorize into a hard subprocess and soft universal hadronic matrix elements. [50, 51, 33] For example, consider exclusive meson electroproduction such as $ep \rightarrow e\pi^+n$ (Fig. 1a). Here one takes (as in DIS) the Bjorken limit of large photon virtuality, with $x_B = Q^2/(2m_p\nu)$ fixed, while the momentum transfer $t = (p_p - p_n)^2$ remains small. These processes involve ‘skewed’ parton distributions, which are generalizations of the usual parton distributions

measured in DIS. The skewed distribution in Fig. 1a describes the emission of a u -quark from the proton target together with the formation of the final neutron from the d -quark and the proton remnants. As the subenergy \hat{s} of the scattering process $\gamma^*u \rightarrow \pi^+d$ is not fixed, the amplitude involves an integral over the u -quark momentum fraction x .

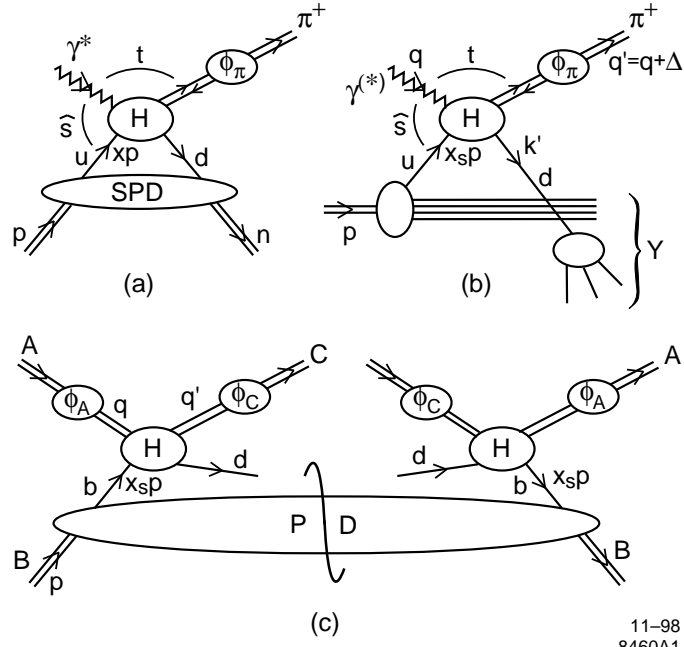
An essential condition for the factorization of the deeply virtual meson production amplitude of Fig. 1a is the existence of a large rapidity gap between the produced meson and the neutron. This factorization remains valid if the neutron is replaced with a hadronic system Y of invariant mass $M_Y^2 \ll W^2$, where W is the c.m. energy of the γ^*p process. For $M_Y^2 \gg m_p^2$ the momentum k' of the d -quark in Fig. 1b is large with respect to the proton remnants, and hence it forms a jet. This jet hadronizes independently of the other particles in the final state if it is not in the direction of the meson, *i.e.*, if the meson has a large transverse momentum $q'_\perp = \Delta_\perp$ with respect to the photon direction in the γ^*p c.m. Then the cross section for an inclusive system Y can be calculated as in DIS, by treating the d -quark as a final state particle.

The large Δ_\perp furthermore allows only transversally compact configurations of the projectile A to couple to the hard subprocess H of Fig. 1b, as it does in exclusive processes. [5] Hence the above discussion applies not only to incoming virtual photons at large Q^2 , but also to real photons ($Q^2 = 0$) and in fact to any hadron projectile.

Let us then consider the general process $A + B \rightarrow C + Y$, where B and C are hadrons or real photons, while the projectile A can also be a virtual photon. In the semi-exclusive kinematic limit $\Lambda_{QCD}^2, M_B^2, M_C^2 \ll M_Y^2, \Delta_\perp^2 \ll W^2$ we have a large rapidity gap $|y_C - y_d| = \log \frac{W^2}{\Delta_\perp^2 + M_Y^2}$ between C and the parton d produced in the hard scattering (see Fig. 1c). The cross section then factorizes into the form

$$\begin{aligned} \frac{d\sigma}{dt dx_S}(A + B \rightarrow C + Y) \\ = \sum_b f_{b/B}(x_S, \mu^2) \frac{d\sigma}{dt}(Ab \rightarrow Cd), \end{aligned} \quad (8)$$

where $t = (q - q')^2$ and $f_{b/B}(x_S, \mu^2)$ denotes the distribution of quarks, anti-quarks and gluons b in the target B . The momentum fraction x_S of the struck parton b is fixed by kinematics to the value $x_S = \frac{-t}{M_Y^2 - t}$ and the factorization scale μ^2 is characteristic of the hard subprocess $Ab \rightarrow Cd$.



11-98
8460A1

Figure 1: (a): Factorization of $\gamma^* p \rightarrow \pi^+ n$ into a skewed parton distribution (SPD), a hard scattering H and the pion distribution amplitude ϕ_π . (b): Semi-exclusive process $\gamma^{(*)} p \rightarrow \pi^+ Y$. The d -quark produced in the hard scattering H hadronizes independently of the spectator partons in the proton. (c): Diagram for the cross section of a generic semi-exclusive process. It involves a hard scattering H , distribution amplitudes ϕ_A and ϕ_C and a parton distribution (PD) in the target B .

It is conceptually helpful to regard the hard scattering amplitude H in Fig. 1c as a generalized current of momentum $q - q' = p_A - p_C$, which interacts with the target parton b . For $A = \gamma^*$ we obtain a close analogy to standard DIS when particle C is removed. With $q' \rightarrow 0$ we thus find $-t \rightarrow Q^2$, $M_Y^2 \rightarrow W^2$, and see that x_S goes over into $x_B = Q^2/(W^2 + Q^2)$. The possibility to control the value of q' (and hence the momentum fraction x_S of the struck parton) as well as the quantum numbers of particles A and C should make semi-exclusive processes a versatile tool for studying hadron structure. The cross section further depends on the distribution amplitudes ϕ_A , ϕ_C (c.f. Fig. 1c), allowing new ways of measuring these quantities. The use of this new current requires a sufficiently high c.m. energy, since we need to have at least one intermediate large scale. The possibility of creating effective currents using processes similar to the ones we discuss here was considered already before the advent of QCD. [49]

In the case of photoproduction one finds in the limit with $Q^2 = 0$ that the $\gamma u \rightarrow \pi^+ d$ subprocess cross section is [3]

$$\begin{aligned} \frac{d\sigma}{dt}(\gamma u \rightarrow \pi^+ d) &= \frac{128\pi^2}{27} \alpha \alpha_s^2 \frac{(e_u - e_d)^2}{\hat{s}^2(-t)} \\ &\times \left\{ \left[\int_0^1 dz \frac{\phi_\pi(z)}{z} \right]^2 + \left[\int_0^1 dz \frac{\phi_\pi(z)}{1-z} \right]^2 \right\}, \end{aligned} \quad (9)$$

where $\int dz \phi_\pi(z) = f_\pi/\sqrt{12}$ with $f_\pi = 93$ MeV. The result for the physical process $\gamma p \rightarrow \pi^+ Y$ is then,

$$\begin{aligned} \frac{d\sigma}{dt dx_S}(\gamma p \rightarrow \pi^+ Y) \\ = \left[u(x_S, -t) + \bar{d}(x_S, -t) \right] \frac{d\sigma}{dt}(\gamma u \rightarrow \pi^+ d) \end{aligned} \quad (10)$$

with the notation $q(x_S, -t) = f_{q/p}(x_S, -t)$. The pion distribution amplitude $\phi_\pi(z)$ enters in precisely the same way as it does in the pion transition form factor for $\gamma^* \gamma \rightarrow \pi^0$ [5, 3]

$$F_{\pi\gamma}(Q^2) = \frac{\sqrt{48}(e_u^2 - e_d^2)}{Q^2} \int_0^1 dz \frac{\phi_\pi(z)}{z}. \quad (11)$$

There are several interesting aspects of this result: Both the target u - and \bar{d} -quark contributions are weighted by the *total charge* $e_u - e_d = +1$ of

the produced π^+ . An analogous formula holds of course if the π^+ is replaced with another pseudoscalar. For neutral meson production, $\gamma p \rightarrow M^0 Y$ with $M^0 = \pi^0, K^0, \eta, \dots$, the expression (9) *vanishes*; more exactly one finds that the cross section is suppressed by $(-t/\hat{s})^2$ compared with the charged meson case. [3] Note that the cross section has a power-law behavior, $d\sigma/dt \propto 1/\hat{s}^3$ at fixed t/\hat{s} . This is the basic signature that the amplitude factorizes into a meson distribution amplitude and a hard scattering subprocess. At fixed t the expression (9) goes like $1/\hat{s}^2$, which is characteristic of two spin 1/2 quark exchanges in the t -channel. Notice that with $\Lambda_{QCD}^2 \ll -t \ll \hat{s}$ the hard scattering takes place in the perturbative Regge regime: if a deviation from this \hat{s} -behavior were to be observed experimentally it would indicate that the quark exchange reggeizes, *i.e.*, that contributions from higher order ladder diagrams are important. At large $-t$, non-singlet Regge trajectories asymptote to 0 or negative integers, reflecting their quark pair composition.[52]

In the semi-exclusive limit with $Q^2 \sim W^2$, and finite x_B , the semi-exclusive electroproduction cross section becomes

$$\begin{aligned} \frac{d\sigma(ep \rightarrow e\pi^+Y)}{dQ^2 dx_B dt dx_S} &= \frac{\alpha}{\pi} \frac{1-y}{Q^2 x_B} \frac{512\pi^2}{27} \alpha_s^2 \frac{x_B}{\hat{s} Q^4 x_S} \\ &\times \left[\int_0^1 dz \frac{\phi_\pi(z)}{z} \right]^2 \left\{ u(x_S) \left[e_u + \left(1 - \frac{x_B}{x_S}\right) e_d \right]^2 \right. \\ &\quad \left. + \bar{d}(x_S) \left[e_d + \left(1 - \frac{x_B}{x_S}\right) e_u \right]^2 \right\} \end{aligned} \quad (12)$$

where $y = \nu/E_e$ is the momentum fraction of the projectile electron carried by the virtual photon, and we have used again $\phi_\pi(z) = \phi_\pi(1-z)$. The semi-exclusive cross section in Eq. (12) corresponds to longitudinal photon exchange. The contribution from transverse photons is suppressed, as in the exclusive case $\gamma^* p \rightarrow Mp$ at large Q^2 and small $-t$. [51]

The systematic comparisons of semi-exclusive photoproduction of various particles at a facility such as EPIC thus can give useful information on parton distributions and distribution amplitudes. The hard subprocess (9) cancels in the ratio of physical cross sections (10) for π^+ and π^- . Hence $d\sigma(\pi^+)/d\sigma(\pi^-)$ directly measures the $(u + \bar{d})/(d + \bar{u})$ parton distribution ratio. Similarly, the $d\sigma(K^+)/d\sigma(K^-)$ ratio measures the strange quark content of the target without uncertainties due, *e.g.*, to fragmentation functions. Conversely, the parton distributions drop out in the ratio $d\sigma(\rho_L^+)/d\sigma(\pi^+)$ of longitudinally polarized ρ mesons to pions, allowing a comparison of their distribution am-

plitudes. Since the normalization of both ϕ_ρ and ϕ_π is fixed by the leptonic decay widths such a comparison can reveal differences in their z -dependence. In the intermediate Q^2 -range the relative size of Q^2 and t can furthermore be tuned to change the dependence of the hard subprocess on z and thus obtain further information on the shape of $\phi(z)$.

Spin and transversity distributions in Semi-Exclusive Reactions. The polarization of the target B can naturally be incorporated in this framework. A longitudinally polarized target selects the usual spin-dependent parton distributions $\Delta q(x_S)$. It also appears possible to measure the quark transverse spin, or transversity distribution in photoproduction of ρ mesons on transversely polarized protons. In this case only the interference term between transversely and longitudinally polarized ρ mesons should contribute.

Color transparency in Semi-Exclusive Reactions. The factorization of the hard amplitude H in Fig. 1c from the target remnants is a consequence of the high transverse momentum which selects compact sizes in the projectile A and in the produced particle C . In the case of nuclear targets this color transparency [53] implies according to Eq. (8) that all target dependence enters via the nuclear parton distribution. Thus tests of color transparency can be made even in photoproduction, *e.g.*, through

$$\gamma A \rightarrow \begin{cases} \pi^+(\Delta_\perp) + Y \\ p(\Delta_\perp) + Y \end{cases} \quad (13)$$

in the semi-exclusive kinematic region. Color transparency has so far been studied mainly in exclusive processes where the target scatters elastically, such as $\gamma^* A \rightarrow \rho A$, [54] $pA \rightarrow pp + (A - 1)$ [55] and $\gamma^* A \rightarrow p + (A - 1)$. Semi-exclusive processes provide a possibility to study color transparency at EPIC where the target dissociates into a heavy inclusive system Y . [56]

6 Odderon-Pomeron Interference at EPIC

The existence of odd charge-conjugation, zero flavor-number exchange contributions to high energy hadron scattering amplitudes is a basic prediction of quantum chromodynamics, following simply from the existence of the color-singlet exchange of three reggeized gluons in the t -channel. [57] In Regge theory, the “Odderon” contribution is dual to a sum over $C = P = -1$ gluonium states in the t -channel. [58, 59] In the case of reactions which involve high momentum transfer, the deviation of the Regge intercept of the Odderon

trajectory from $\alpha_{\mathcal{O}}(t=0) = 1$ can in principle be computed [60, 61, 62, 63] from perturbative QCD in analogy to the methods used to compute the properties of the hard BFKL pomeron.[64]

Recently Rathsmann, Merino and I [7] have proposed an experimental test well suited to EPIC, COMPASS, and HERA kinematics which should be able to disentangle the contributions of both the Pomeron and the Odderon to diffractive production of charmed jets. By forming a charge asymmetry in the energy of the charmed jets, we can determine the relative importance of the Pomeron ($C = +$) and the Odderon ($C = -$) contributions, and their interference, thus providing a new experimental test of the separate existence of these two objects. Since the asymmetry measures the Odderon amplitude linearly, even a relatively weakly-coupled amplitude should be visible.

The leading contributions to the amplitude for diffractive photoproduction of a charm quark anti-quark pair is given by single Pomeron exchange (two reggeized gluons), and the next term in the Born expansion is given by the exchange of one Odderon (three reggeized gluons). In general the Pomeron and Odderon exchange amplitudes will interfere. The contribution of the interference term to the total cross-section is zero, but it does contribute to charge-asymmetric rates. Thus we propose the study of photoproduction of $c\bar{c}$ pairs and measure the asymmetry in the energy fractions z_c and $z_{\bar{c}}$. More generally, one can use other charge-asymmetric kinematic configurations, as well as bottom or strange quarks. The interference term can be isolated by forming the charge asymmetry,

$$\mathcal{A}(t, M_X^2, z_c) = \frac{\frac{d\sigma}{dtdM_X^2 dz_c} - \frac{d\sigma}{dtdM_X^2 dz_{\bar{c}}}}{\frac{d\sigma}{dtdM_X^2 dz_c} + \frac{d\sigma}{dtdM_X^2 dz_{\bar{c}}}}, \quad (14)$$

The predicted asymmetry has the form

$$\begin{aligned} & \mathcal{A}(t, M_X^2, z_c) \\ &= \frac{g_{pp'}^{\mathcal{P}} g_{pp'}^{\mathcal{O}} \left(\frac{s_{\gamma p}}{M_X^2} \right)^{\alpha_{\mathcal{P}} + \alpha_{\mathcal{O}}} \frac{2 \sin \left[\frac{\pi}{2} (\alpha_{\mathcal{O}} - \alpha_{\mathcal{P}}) \right]}{\sin \frac{\pi \alpha_{\mathcal{P}}}{2} \cos \frac{\pi \alpha_{\mathcal{O}}}{2}} g_{\mathcal{P}}^{\gamma c \bar{c}} g_{\mathcal{O}}^{\gamma c \bar{c}}}{\left[g_{pp'}^{\mathcal{P}} \left(\frac{s_{\gamma p}}{M_X^2} \right)^{\alpha_{\mathcal{P}}} g_{\mathcal{P}}^{\gamma c \bar{c}} / \sin \frac{\pi \alpha_{\mathcal{P}}}{2} \right]^2 + \left[g_{pp'}^{\mathcal{O}} \left(\frac{s_{\gamma p}}{M_X^2} \right)^{\alpha_{\mathcal{O}}} g_{\mathcal{O}}^{\gamma c \bar{c}} / \cos \frac{\pi \alpha_{\mathcal{O}}}{2} \right]^2}. \end{aligned} \quad (15)$$

Thus by observing the charge asymmetry of the charm quark/antiquark energy fraction (z_c) in diffractive $c\bar{c}$ pair photoproduction, the interference

between the Pomeron and the Odderon exchanges can be isolated and the ratio to the sum of the Pomeron and the Odderon exchanges measured. In a simple model for the Pomeron/Odderon coupling to the photon the asymmetry is predicted to be proportional to $(2z_c - 1)/(z_c^2 + (1 - z_c)^2)$ and the magnitude is of order 15% (and possibly significantly larger for diffractive proton dissociation). Such a test could be performed by experiments at EPIC, COMPASS, or HERA measuring the diffractive production of open charm in photoproduction or electroproduction. Such measurements could provide the first experimental evidence for the existence of the Odderon, as well as the relative strength of the Odderon and Pomeron couplings. Most important, the energy dependence of the asymmetry can be used to determine whether the Odderon intercept is in fact greater or less than that of the Pomeron.

7 Summary

An electron-proton/ion polarized beam collider of medium energy clearly has strong potential for future fundamental studies of proton and nuclear structure in QCD. Only a sample of EPIC topics have been highlighted here, such as semi-exclusive reactions, studies of the proton fragmentation region, heavy quark studies, and odderon/pomeron interference.

I thank my collaborators, particularly Johan Rathsmann, Carlos Merino, Paul Hoyer, Stephane Peigne, and Markus Diehl, for many helpful discussions. I also thank the organizers of this meeting at the Indiana University Cyclotron Facility for stimulating and organizing this interesting workshop.

References

- [1] P. J. Mulders, hep-ph/9905563, and these proceedings.
- [2] L. Trentadue and G. Veneziano, *Phys. Lett.* **B323**, 201 (1994).
- [3] C. E. Carlson and A. B. Wakely, *Phys. Rev.***D48**, 2000 (1993); A. Afanasev, C. E. Carlson and C. Wahlquist, *Phys. Lett.***B398**, 393 (1997), hep-ph/9701215 and *Phys. Rev.***D58**, 054007 (1998), hep-ph/9706522.
- [4] S. J. Brodsky, M. Diehl, P. Hoyer and S. Peigne, *Phys. Lett.* **B449**, 306 (1999) hep-ph/9812277.
- [5] G. P. Lepage and S. J. Brodsky, *Phys. Rev.* **D22**, 2157 (1980); S. J. Brodsky and G. P. Lepage, *Phys. Rev.***D24**, 1808 (1981). For reviews and further references to exclusive processes in QCD, see S. J. Brodsky and G. P. Lepage, in: *Perturbative Quantum Chromodynamics*, ed. A. H. Mueller (World Scientific, Singapore, 1989); V. L. Chernyak and A. R. Zhitnitsky, *Phys. Rept.***122**, 173 (1984).
- [6] A.V. Efremov and A.V. Radyushkin, *Phys. Lett.* **94B**, 245 (1980).
- [7] S. J. Brodsky, J. Rathsman and C. Merino, hep-ph/9904280.
- [8] S. J. Brodsky and A.H. Mueller, *Phys. Lett.* **206B**, 685 (1988).
- [9] L. Frankfurt and M. Strikman, *Prog. Part. Nucl. Phys.* **27**, 135 (1991).
- [10] S. Heppelmann, *Nucl. Phys. B (Proc. Suppl.)* **12**, 159 (1990), and references therein.
- [11] B. Blaettel, G. Baym, L. L. Frankfurt, H. Heiselberg, and M. Strikman, *Phys. Rev.* **D47**, 2761 (1993).
- [12] S. J. Brodsky, C.-R. Ji, and G. P. Lepage, *Phys. Rev. Lett.* **51**, 83 (1983).
- [13] S. J. Brodsky, P. Hoyer, C. Peterson, and N. Sakai, *Phys. Lett.* **93B**, 451 (1980).
- [14] B. W. Harris, J. Smith, and R. Vogt, *Nucl. Phys.* **B461**, 181 (1996), hep-ph/9508403.
- [15] S. J. Brodsky, F. E. Close and J. F. Gunion, *Phys. Rev.* **D6**, 177 (1972).

- [16] S.J. Brodsky, F.E. Close and J.F. Gunion, *Phys. Rev.* **D8**, 3678 (1973).
- [17] S. J. Brodsky, J. F. Gunion and R. Jaffe, *Phys. Rev.* **D6**, 2487 (1972).
- [18] For a review of light-cone Hamiltonian methods and further references, see S. J. Brodsky, H. C. Pauli, and S. S. Pinsky, *Phys. Rept.* **301**, 299 (1998). See also the lectures: S. Brodsky, SLAC-PUB-7645, hep-ph/9710288.
- [19] G. Bertsch, S. J. Brodsky, A. S. Goldhaber, and J. F. Gunion, *Phys. Rev. Lett.* **47**, 297 (1981).
- [20] L. Frankfurt, G. A. Miller, and M. Strikman, *Phys. Lett.* **B304**, 1 (1993), hep-ph/9305228.
- [21] S. J. Brodsky and S. D. Drell, *Phys. Rev.* **D22**, 2236 (1980).
- [22] S.J. Brodsky and D.S. Hwang, *Nucl. Phys.* **B543**, 239 (1999) hep-ph/9806358.
- [23] H. C. Pauli and S. J. Brodsky, *Phys. Rev.* **D32**, 2001 (1985).
- [24] S. J. Brodsky and H. C. Pauli, SLAC-PUB-5558, published in Schladinger 1991, Proceedings.
- [25] A. Szczepaniak, E. M. Henley and S. J. Brodsky, *Phys. Lett.* **B243**, 287 (1990).
- [26] A. Szczepaniak, *Phys. Rev.* **D54**, 1167 (1996).
- [27] P. Ball, *JHEP* 9809:005 (1998); hep-ph/9803501 (1998).
- [28] P. Ball and V. M. Braun, *Phys. Rev.* **D58**, 094016 (1998).
- [29] S. J. Brodsky, C.-R. Ji, A. Pang, and D. G. Robertson, SLAC-PUB-7473, *Phys. Rev.* **D57**, 245 (1998), hep-ph/9705221.
- [30] D. Ashery, *et al.*, Fermilab E791 Collaboration, to be published.
- [31] P. Kroll and M. Raulfs, *Phys. Lett.* **B387**, 848 (1996).
- [32] I. V. Musatov and A. V. Radyushkin, *Phys. Rev.* **D56**, 2713 (1997).

- [33] S. J. Brodsky, L. Frankfurt, J. F. Gunion, A. H. Mueller, and M. Strikman, *Phys. Rev.* **D50**, 3134 (1994).
- [34] F. Antonuccio, S. J. Brodsky, and S. Dalley, *Phys. Lett.* **B412**, 104 (1997).
- [35] A. H. Mueller, *Nucl. Phys.* **B415**, 373 (1994).
- [36] D. Mueller, SLAC-PUB-6496, May 1994, hep-ph/9406260.
- [37] S. J. Brodsky and I. A. Schmidt, *Phys. Lett.* **B234**, 144 (1990).
- [38] S. J. Brodsky, P. Hoyer, A. H. Mueller, W.-K. Tang, *Nucl. Phys.* **B369**, 519 (1992).
- [39] S. J. Brodsky and A. Mueller, Ref. [8]. R. Vogt, S. J. Brodsky, and P. Hoyer, *Nucl. Phys.* **B360**, 67 (1991); *Nucl. Phys.* **B383**, 643 (1992).
- [40] P. Hoyer and S. Peigne, *Phys. Rev.* **D59**, 034011 (1999).
- [41] E. L. Berger and S. J. Brodsky, *Phys. Rev. Lett.* **42**, 940 (1979).
- [42] A. Brandenburg, S. J. Brodsky, V.V. Khoze, and D. Mueller, *Phys. Rev. Lett.* **73**, 939 (1994).
- [43] A. I. Signal and A. W. Thomas, *Phys. Lett.* **B 191**, 205 (1987). M. Burkardt and B. J. Warr, *Phys. Rev.* **D 45**, 958 (1992).
- [44] S. J. Brodsky and B.-Q. Ma, *Phys. Lett.* **B381**, 317 (1996).
- [45] S. J. Brodsky and B. T. Chertok, *Phys. Rev.* **D14**, 3003 (1976).
- [46] G. R. Farrar, K. Huleihel, and H. Zhang, *Phys. Rev. Lett.* **74**, 650 (1995).
- [47] A. D. Krisch, *Nucl. Phys. B (Proc. Suppl.)* **25**, 285 (1992).
- [48] S. J. Brodsky and G. F. de Teramond, *Phys. Rev. Lett.* **60**, 1924 (1988).
- [49] J. F. Gunion, S. J. Brodsky and R. Blankenbecler, *Phys. Rev.* **bf D6**, 2652 (1972); R. Blankenbecler and S. J. Brodsky, *Phys. Rev.* **D10**, 2973 (1974).

- [50] X. Ji, *Phys. Rev.***D55**, 7114 (1997), hep-ph/9609381; X. Ji and J. Osborne, *Phys. Rev.***D58**, 094018 (1998), hep-ph/9801260; A.V. Radyushkin, *Phys. Rev.***D56**, 5524 (1997), hep-ph/9704207.
- [51] J. C. Collins, L. Frankfurt and M. Strikman, *Phys. Rev.***D56**, 2982 (1997).
- [52] S. J. Brodsky, W.-K. Tang and C. B. Thorn, *Phys. Lett.***B318**, 203 (1993).
- [53] S. J. Brodsky and A. H. Mueller, Ref. [8]; L. Frankfurt and M. Strikman, *Phys. Rept.* **160** , 235 (1988); P. Jain, B. Pire and J. P. Ralston, *Phys. Rept.* **271**, 67(1966).
- [54] M. R. Adams, *et al.*, *Phys. Rev. Lett.* **74**, 1525 (1995).
- [55] R. S. Carroll *et al.*, *Phys. Rev. Lett.* **61**, 1698 (1988).
- [56] P. Hoyer, *Nucl. Phys.***A622**, 284c (1997).
- [57] J. Kwiecinski and M. Praszalowicz, *Phys. Lett.* **94B**, 413 (1980); J. Bartels, *Nucl. Phys.* **B 175**, 365 (1980).
- [58] P.V. Landshoff and O. Nachtmann, hep-ph/9808233.
- [59] L. Lukaszuk and B. Nicolescu, *Nuovo Cimento Letters* **8**, 405 (1973).
- [60] P. Gauron, L.N. Lipatov, and B. Nicolescu, *Z. Phys.***C63**, 253 (1994).
- [61] N. Armesto and M.A. Braun, *Z. Phys.***C75**, 709 (1997).
- [62] R.A. Janik and J. Wosieck, *Phys. Rev. Lett.* **82**, 1092 (1999).
- [63] M.A. Braun, P. Gauron, and B. Nicolescu, *Nucl. Phys.* **B542**, 329 (1999).
- [64] E.A. Kuraev, L.N. Lipatov, and V.S. Fadin, *Sov. Phys. JETP* **44** (1976) 443; *Sov. Phys. JETP* **45**, 199 (1977). Y.Y. Balitski and L.N. Lipatov, *Sov. J. Nucl. Phys.* **28**, 822 (1978).